BULLETIN OF THE CHEMICAL SOCIETY OF JAPAN, VOL. 50 (4), 802—809 (1977)

Calorimetric Study of the Glassy State. XI. Plural Glass Transition Phenomena of Cyclohexene

Osamu Haida, Hiroshi Suga, and Syûzô Seki

Department of Chemistry, Faculty of Science, Osaka University, Toyonaka, Osaka 560

(Received October 14, 1976)

Two kinds of glassy crystalline phases (I and III) of cyclohexene were realized by different thermal treatments. The heat capacities of the glassy and the supercooled crystal-I and -III, as well as the stable crystalline phases were measured by an adiabatic calorimeter in the temperature range 12—300 K. The glass transition temperature T_g, the heat capacity jump at T_g and the residual entropy were found to be 81 K, 11.4 JK^{-1} mol^{-1} and 11.7 JK^{-1} mol^{-1} for crystal-I and 83 K, 3.6 JK^{-1} mol^{-1} and 2.6 JK^{-1} mol^{-1} for crystal-III, respectively. The glassy liquid state of cyclohexene was realized by vapor condensation technique, its T_g being 78 K as determined by DTA method. The results provide the first example of plural glass transition phenomena in one and the same low-molecular-weight compound.

The heat capacity of liquid contains a contribution from a potential energy variation caused by structural change with temperature. This degree of freedom is usually known as "configurational freedom" and has been used in many theoretical works for describing the thermal behavior of glass-forming liquid in a transfigured fashion such as free volume,[1] trans-gauche conformation[2] and bond-lattice model.[3] These treatments have been successful to a certain extent to explain thermodynamic and kinetic aspects of the glass transition in spite of their simplified models.

Discovery of glassy crystals[4] brought about an extension of the concept of glass from the originally defined non-equilibrium frozen state of liquid to that of a system including some kind of disorder. In addition it offers a new possibility for studying the glassy state. The site randomness will be eliminated from the configurational freedom in the case of glassy crystals since they have three-dimensional positional periodicity. Even in this favorable situation, however, the "configuration" is of a complex mixture of orientational and internal freedom of molecule, as pointed out by Adachi *et al.*[4] The realization of more than one kind of glassy state of a compound is therefore expected to give a clue in resolving the entanglement between these freedoms.

The calorimetric study by Huffman *et al.*[5] revealed the fact that cyclohexene has two crystalline phases, I and II. Adachi *et al.*[6] realized the glassy state of high temperature crystalline phase I based on the results of DTA experiment. We have found a new crystalline phase (crystal-III) and its glassy crystalline state. The glassy liquid state of cyclohexene was also realized by the vapor condensation method. A brief account of these findings was reported in a short communication.[7]

Experimental

Material. Commercial "Standard Material" of cyclohexene (Tokyo Kagaku Seiki Co., Ltd.) was deaerated and then distilled twice in a vacuun. The final purity of the sample was determined to be 99.98% by gas chromatography (Shimadzu Gas Chromatogram G.C./C. column; Apiezon grease on serite, column temperature; 70 °C) and 99.96% by calorimetric study.

Apparatus. The heat capacity was measured with an adiabatic calorimeter.[8] The purified sample was introduced into the calorimeter cell by vacuum distillation through a copper tubing attached to the top of the cell. When the procedure was over, the cell was pinched off at the copper tubing and sealed with a soft solder. The weight of the sample used for the heat capacity measurement was 23.154 g.

The DTA apparatus used in the preparation of the glassy liquid has also been reported.[9]

Experimental Results

DTA. The thermal behavior of cyclohexene at low temperature was examined by use of DTA, the results being given in Fig. 1. Run 1 shows the cooling curve with a rate of $-2\ K\ min^{-1}$, and Run 2 the subsequent heating curve. Run 3 shows the heating curve of rapidly cooled sample at a rate greater than $7\ K\ min^{-1}$ from high temperature crystal-I or liquid. The result of Run 3 coincides with that reported previously[6] except for a difference in anomalies at 120 and 140 K. The endothermic peaks at 140 K in Run 3 and 170 K in Runs 2 and 3 correspond to the processes crystal-I→crystal-II and crystal-II→liquid, respectively. When the liquid is cooled slowly as in Run 1, it crystallizes into crystal-I at around 130 K with successive two exothermic effects, and then the crystal-I transforms into a newly found crystal-III reversibly at about 115 K. The successive peaks at 130 K in Run 1 were separated

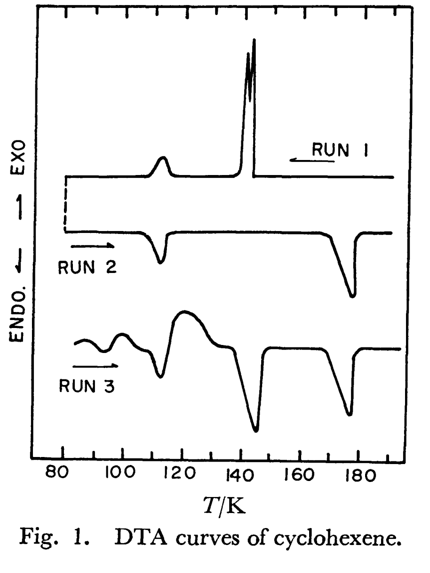

Fig. 1. DTA curves of cyclohexene.

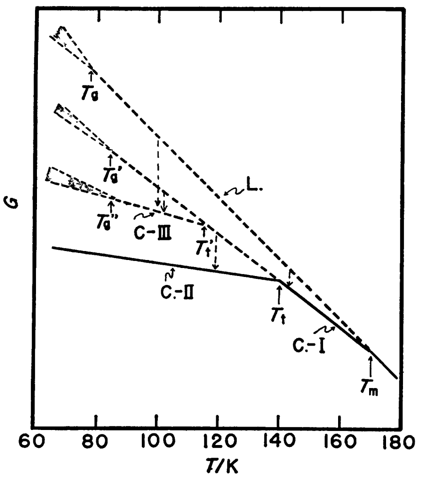

Fig. 2. Schematic diagram for Gibbs energy relationship of cyclohexene.

by chance and might be attributed to the appearance of a metastable phase on the way from liquid into crystal-I.

The thermogram Run 3 is interpreted as follows. When crystal-I is chilled through the transition temperature (115 K) at a rate greater than $-7\ \mathrm{K\ min^{-1}}$, the glassy crystal-I can be prepared. During the course of subsequent heating, the glassy crystal-I recrystallizes into crystal-III at *ca.* 100 K after the glass transition at 92 K is over, and then successive transformations of crystal-III→crystal-I→crystal-II→crystal-I→liquid take place at 115, 120, 140, and 160 K, respectively. This interpretation was confirmed by calorimetric studies. Among the transitions in Run 3 the rate of irreversible transition from crystal-I to crystal-II at 120 K was found to be sensitive to the purity and thermal history of the specimen. Thus a different thermal behavior in the temperature range 120—140 K is seen in the results of Runs 2 and 3 (Fig. 1), Runs 2, 3, and 4 (Fig. 6) and those reported by Adachi *et al.*[6] The phase relations represented by Gibbs energy are schematically illustrated in Fig. 2. Glassy state of liquid (glassy liquid) was obtained by vapor condensation method, but not by rapid cooling method. This can be seen from the fact that the samples quenched from liquid and crystal-I gave the same thermogram Run 3.

Measurement of Heat Capacity. Glassy crystal-I was prepared by rapid chilling of the liquid sample by introducing liquid nitrogen directly into the calorimeter can. The average cooling rate in the temperature interval 220—80 K was *ca.* $-40\ \mathrm{K\ min^{-1}}$, which is much greater than the limit $-7\ \mathrm{K\ min^{-1}}$ to obtain the thermogram Run 3 (Fig. 1). Concerning the crystal-III, series of measurement were performed with different samples. Thermal treatments adopted to obtain these samples were as follows. For series-I, crystal-III was prepared by cooling crystal-I at the cooling rate of *ca.* $-1\ \mathrm{K\ min^{-1}}$; for series-2 crystal-III (obtained by the same procedure as series-I) was annealed at 78 K for *ca.* 36 h; for series-3, it was made through the phase transformation from crystal-I (on which the heat capacity measurement up to 100 K was carried out) and subsequent annealing at 80—100 K for about 2 days. Crystal-II was prepared by cooling the crystal-I to 78 K and subsequent annealing at *ca.* 120 K. Complete transformation of crystal-I into crystal-II was confirmed by observing the cessation of the heat evolution accompanied by irreversible phase transition.

The molar heat capacities are given in Table 1 and plotted in Fig. 3. Besides the big heat capacity jump due to the glass transition phenomenon of crystal-I, a small heat capacity jump for crystal-III at *ca.* 80 K can also be seen. In the measurement for crystal-I and -III, heat evolution was observed in the temperature range

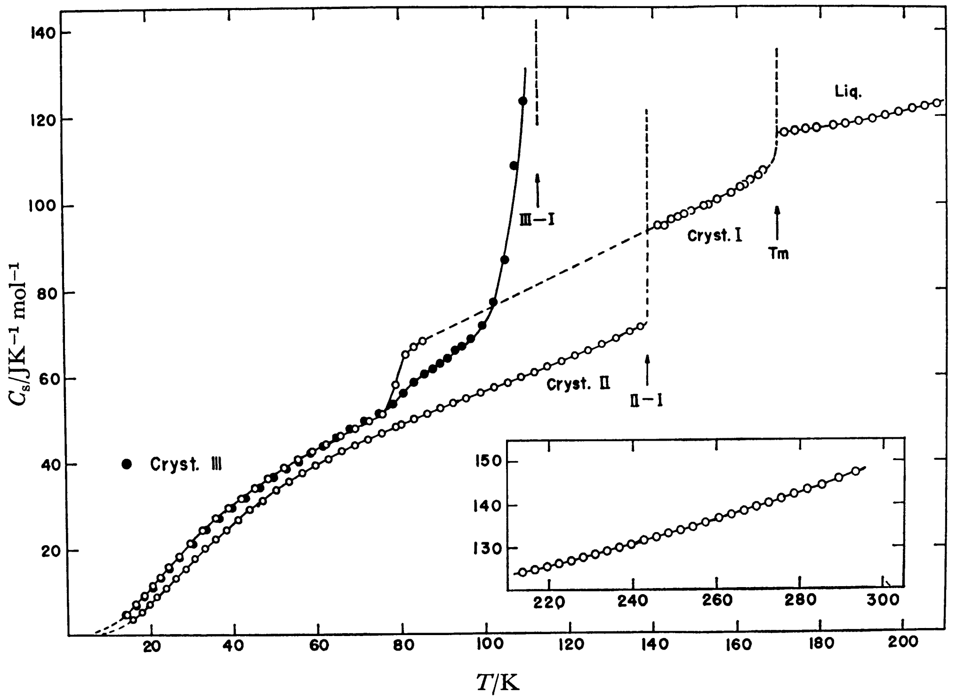

Fig. 3. Heat capacity curves of cyclohexene.

TABLE 1. MOLAR HEAT CAPACITY OF CYCLOHEXENE
mol wt=82.147 0 °C=273.15K

T_{av} / K	$\Delta H/\Delta T$ / $JK^{-1}\,mol^{-1}$	ΔT / K
	Crystal-II	
15.63	3.580	2.372
17.86	5.294	2.081
19.87	7.057	1.918
21.78	8.792	1.884
23.76	10.86	2.064
26.03	13.06	2.456
28.41	15.48	2.314
30.77	17.83	2.414
33.22	20.20	2.485
35.74	22.47	2.542
38.35	24.59	2.694
41.09	26.86	2.774
43.89	29.28	2.839
46.94	31.38	3.252
50.16	33.74	3.184
53.32	35.70	3.149
56.46	37.54	3.129
59.61	39.32	3.164
62.71	40.86	3.037
65.83	42.71	3.203
68.98	44.04	3.101
72.17	45.45	3.277
75.44	46.89	3.265
78.68	48.32	3.217
79.92	48.81	2.920
82.98	50.14	3.208
86.15	51.48	3.128
89.24	52.70	3.063
92.28	53.81	3.005
95.46	54.93	3.354
98.78	56.13	3.290
102.04	57.33	3.244
105.25	58.48	3.176
108.40	59.65	3.123
111.52	60.78	3.091
114.72	62.00	3.313
118.01	63.25	3.254
121.23	64.50	3.202
124.40	65.74	3.124
127.66	67.13	3.402
131.03	68.55	3.345
134.35	70.06	3.290
136.81	71.27	1.623
Glassy and supercooled crystal-I		
14.25	4.744	2.127
16.41	7.170	2.200
18.40	9.086	1.898
20.53	11.44	2.048
22.38	13.45	1.660
24.33	15.77	2.246
26.79	18.47	2.676
29.63	21.47	2.992
32.68	24.50	3.113
35.83	27.33	3.194
38.87	29.58	2.879
41.98	31.83	3.332
45.19	34.18	3.092
48.40	36.40	3.317
52.15	38.78	3.092
55.46	40.73	3.514
58.89	42.53	3.348
62.17	44.36	3.204
65.55	46.25	3.531
69.02	47.95	3.399
72.37	49.62	3.282
75.61	51.30	3.179
78.65	58.04	2.909
81.00	65.01	1.791
82.99	66.77	2.183
85.15	68.15	2.143
	Crystal-I (series 1)	
140.94	94.84	3.269
144.19	96.08	3.234
147.40	97.44	3.196
150.57	99.17	3.151
153.72	99.66	3.135
	(series 2)	
142.68	94.81	3.161
145.82	96.75	3.112
148.91	98.09	3.077
151.97	99.44	3.041
155.17	100.86	3.344
158.49	102.40	3.302
161.77	104.22	3.256
165.00	106.35	3.206
	Glassy crystal-III and crystal-III	
14.29	4.747	2.178
16.50	6.858	2.257
18.50	8.877	1.742
20.50	10.95	2.244
22.57	13.21	1.952
24.58	15.39	2.127
27.08	18.10	2.872
30.29	21.19	3.548
33.58	24.55	3.031
36.74	27.23	3.284
39.87	29.58	2.983
43.00	31.95	3.267
46.32	36.37	3.385
49.60	36.57	3.167
52.70	38.59	2.985
58.40	42.10	2.722
61.35	43.79	3.160
64.45	45.81	3.023
67.75	47.83	3.577
71.27	49.68	3.445
74.66	51.46	3.327
77.93	53.64	3.207
80.55	56.07	2.061
83.05	58.70	2.987
85.50	60.45	1.926
87.43	61.72	1.920

Table 1. (Continued)

$\frac{T_{av}}{\text{K}}$	$\frac{\Delta H/\Delta T}{\text{JK}^{-1}\,\text{mol}^{-1}}$	$\frac{\Delta T}{\text{K}}$
89.27	62.96	1.757
91.01	64.09	1.723
92.75	65.99	1.661
94.47	66.84	1.874
96.66	68.54	2.394
99.25	71.71	2.819
101.99	77.19	2.657
104.73	87.09	2.421
107.13	108.65	2.771
109.29	123.41	1.543
	(series 2)	
81.51	57.26	2.906
84.37	59.61	2.812
87.14	61.43	2.730
89.84	62.99	2.676
	(series 3)	
79.07	55.44	2.275
80.99	57.40	1.570
82.68	58.62	1.799
84.46	59.80	1.770
86.22	60.89	1.742
87.95	62.08	1.715
	Liquid	
171.17	116.1	2.574
173.74	116.5	2.565
176.31	116.9	2.557
177.38	116.9	2.756
178.97	117.1	2.757
180.14	117.3	2.746
182.88	117.8	2.734
185.87	118.2	3.237
189.09	118.8	3.223
192.30	119.4	3.205
195.45	120.0	3.190
198.68	120.6	3.175
201.85	121.2	3.161
204.83	121.9	2.968
207.79	122.5	2.953
210.73	123.2	2.937
213.66	123.8	2.923
216.58	124.5	2.909
219.48	125.2	2.897
222.37	125.8	2.883
225.24	126.6	2.870
228.11	127.3	2.856
230.96	128.0	2.842
233.82	128.8	2.911
236.73	129.6	2.895
239.66	130.3	2.967
242.61	131.2	2.949
245.56	132.1	2.934
248.48	132.9	2.922
251.40	133.6	2.904
257.37	135.4	3.304
260.53	136.4	3.031
263.55	137.2	3.016
266.56	138.0	3.000
269.53	139.1	2.979
272.50	139.9	2.967
275.54	140.9	3.127
278.66	141.9	3.108
281.76	142.9	3.089
285.35	143.9	4.096
289.42	145.4	4.061
293.43	146.8	4.030

53—78 K. The effect of this heat evolution due to stabilization was removed from heat capacity values by correcting the temperature drift. At temperatures near 80 K, the temperature drift was followed for half an hour after the energy input was over. The last temperature observed was used as the final temperature for the calculation of heat capacity. Thus, these values correspond to the heat capacities for the time scale of 1/2 h. The heat capacity we obtained was compared with the data of Huffman *et al.*[5] Their data are 0.3—0.5% greater for liquid and 0.2—0.8% greater for crystal-I. For crystal-II, they are about 0.5% greater at temperatures near the melting point.

Studies on Phase Transitions. *a) Crystal-II→ Crystal-I Phase Transition*: This phase transition is of a sluggish nature.[5] In order to determine the transition temperature, the electric energy for the completion of transition was added to the sample in eight separate stages, the temperature drift being followed each time for 2 h or more after the energy input was over. The temperature drift did not cease even after 2 h. The temperature after 2 h was observed to decrease in the first three stages. The temperature drift for 3rd and 4th energy inputs was analyzed by means of exponential function and the equilibrium temperature was estimated. Since the value coincides within 25/10000 K, we adopt it as the transition temperature. Heat of transition was measured twice, the results being given in Table 2 together with those of Huffman *et al.*

b) Fusion: The equilibrium temperature during the course of fusion was measured as a function of fraction melted. Assuming no solid solution formation, the

Table 2. Molar heat of transition (Crystal-II → Crystal-I)

$T_t=138.63\pm0.003$ K	
	$\Delta_t H$/kJ mol^{-1}
Experiment 1	4.228
Experiment 2	4.235
mean	4.231 ± 0.003
$\Delta_t S=30.53\pm0.03$ JK^{-1} mol^{-1}	
Huffman *et al.*	
$T_t=138.7\pm0.2$ K	$\Delta_t H=4.251\pm0.004$ kJ mol^{-1}

TABLE 3. MOLAR HEAT OF FUSION

$T_{\mathrm{t.p.}}=169.66\pm0.01$ K	
	$\Delta_m H$/kJ mol^{-1}
Experiment 1	3.282
Experiment 2	3.286
mean	3.284±0.002
$\Delta_m S=19.36\pm0.01$ JK^{-1} mol^{-1}	
Huffman *et al.*	
$T_{\mathrm{t.p.}}=169.67\pm0.05$ K	$\Delta_m H=3.293\pm0.002$ kJ mol^{-1}

purity of the specimen was determined to be 99.96%. The heat of fusion was measured twice (Table 3).

c) Crystal-III→Crystal-I Phase Transition: Since a rather long time (an hour or more) was necessary to obtain one heat capacity data, an irreversible phase transition from the newly formed crystal-I into crystal-II inevitably began during the measurement of crystal-III →crystal-I transition. The transition temperature and the molar heat of transition ($\Delta_{\mathrm{III-I}}H$) were determined as follows: Crystal-III was heated by electric energy from T_{i} to a temperature at which the crystal-III was transformed almost completely into crystal-I. The spontaneous temperature rise due to the irreversible phase transition from crystal-I to crystal-II was then followed. When the transition was almost completed, the electric energy was further supplied to the sample in order to bring it into crystal-I, the final temperature being T_{f}. This last procedure was necessary because the final stage of the transition (metastable crystal-I→ crystal-II) was so sluggish that it caused a large error due to the heat leak during the time consuming observation for detecting the end point of transition. The value $\Delta_{\mathrm{III-I}}H$ can be calculated by means of the following relations.

$$\Delta_{\mathrm{III-I}}H = H^{\mathrm{I}}_{T_{\mathrm{t}}} - H^{\mathrm{III}}_{T_{\mathrm{t}}} \tag{1}$$

$$H^{\mathrm{I}}_{T_{\mathrm{t}}} = H^{\mathrm{I}}_{T_{\mathrm{m}}} - \int_{T_{\mathrm{t}}}^{T_{\mathrm{m}}} C^{\mathrm{I}}_{p}\mathrm{d}T \tag{2}$$

$$H^{\mathrm{III}}_{T_{\mathrm{t}}} = H^{\mathrm{I}}_{T_{\mathrm{t}}} + \int_{T_{\mathrm{i}}}^{T_{\mathrm{t}}} C^{\mathrm{III}}_{p}\mathrm{d}T - E \tag{3}$$

where T_{t} is the transition point of crystal-III→crystal-I, T_{m} the melting point, $C_p{}^{\mathrm{I}}$, $C_p{}^{\mathrm{III}}$ the extrapolated values of heat capacity of crystals I and III, respectively, and E the total energy input. In Eqs. 1, 2 and 3 the terms for the empty cell are omitted for the sake of simplicity. The approximation that the whole of $\Delta_{\mathrm{I-III}}H$ is absorbed at $T=T_{\mathrm{t}}$ is also involved implicity. The data and equations used for calculating $\Delta_{\mathrm{III-I}}H$ are summarized in Table 4. Because of the spontaneous recrystallization, the heat capacity measurement for crystal-I was intervened between 85 and 139 K. The heat capacities in this range were estimated by means of the equation given in Table 4, calculated by extrapolating the measured heat capacities between 140 and 152 K and bringing the result to fit smoothly the data around 85 K.

TABLE 4. TRANSITION (Crystal-III→Crystal-I) DATA SUMMARY

$T_{\mathrm{t}}=112.3\pm0.1$ K
$\Delta_{\mathrm{t}}H=1.483\pm0.054$ kJ mol^{-1}
$\Delta_m S=13.72\pm0.45$ JK^{-1} mol^{-1}

$$\left(\begin{array}{l} C_p{}^{\mathrm{I}}=32.19+0.4437\ T \\ C_p{}^{\mathrm{III}}=3.60+0.6650\ T \\ T_{\mathrm{i}}=99.9117\ \mathrm{K} \\ T_{\mathrm{f}}=141.5663\ \mathrm{K} \\ E=1830.84\ \mathrm{J} \end{array}\right)$$

On the other hand, the transition temperature was determined by the dynamical method. Electric energy was put into the crystal-III at a constant rate and the time variation of temperature was followed. Transition temperature was determined to be the temperature where $\mathrm{d}T/\mathrm{d}t$ (T; temperature, t; time) attained minimum value. The temperature difference between temperature during the energy input and that corresponding to the equilibrium state was corrected by measuring the difference at lower temperatures at which no phase transition effect takes place.

Residual Entropy of Glassy Crystalline States. Beckett *et al.*[10] calculated the entropy and heat capacity of ideal gas state of cyclohexene on the basis of spectroscopic data. Although spectroscopic entropy coincided with the experimental one within their error limits, there was a significant difference between the calculated and the observed heat capacity data. They explained the difference by assuming the existence of an energy-rich conformer having a larger strain energy (11.3 kJ mol^{-1}) than that of the ordinary half-chair conformer. Since the discrepancy for entropy (0.16 JK^{-1} mol^{-1}) is within experimental error, it might be that the crystal-II has

TABLE 5. THIRD LAW ENTROPY OF CRYSTAL-I AT 138.63 K

T/K		ΔS/JK^{-1}mol^{-1}
Via II-I transition		
0—14.0	Debye extrapolation ($\theta_{\mathrm{D}}=157.4$ K, 6 freedom)	0.91
14.0—138.63	$\int C_p(\mathrm{II})/T\,\mathrm{d}T$ (graphical)	71.12
138.63	II-I transition 4231/138.63	30.53
		102.56±0.17
Via Glassy Crystal-I		
0—14.0	Debye extrapolation ($\theta_{\mathrm{D}}=129.4$ K, 6 freedom)	1.62
14.0—86.0	$\int C_p(\mathrm{I})/T\,\mathrm{d}T$ (graphical)	50.53
86.0—138.63	$\int C_p(\mathrm{I})^{\mathrm{a)}}/T\,\mathrm{d}T$	38.74
		90.89±0.63
Via Glassy Crystal-III		
0—14.0	Debye extrapolation ($\theta_{\mathrm{D}}=131.1$ K, 6 freedom)	1.55
14.0—90.0	$\int C_p(\mathrm{III})/T\,\mathrm{d}T$	51.94
90.0—112.3	$\int C_p(\mathrm{III})/T\,\mathrm{d}T$	15.63
	III-I transition	13.72
112.3—138.63	$\int C_p\,(\mathrm{I})/T\,\mathrm{d}T$	17.11
		99.95±0.20

$S_0{}^\circ(\mathrm{I})=102.56-90.89=11.67\pm0.70$ JK^{-1} mol^{-1}
$S_0{}^\circ(\mathrm{III})=102.56-99.95=2.61\pm0.37$ JK^{-1} mol^{-1}

a) Estimated heat capacity given in Table 4.

Table 6. Thermodynamic functions of cyclohexene

T / K	C_s° / JK^{-1} mol^{-1}	S_s° / JK^{-1} mol^{-1}	$(H^\circ - H_0^\circ(\mathrm{I}))/T$ / JK^{-1} mol^{-1}	$-(G^\circ - H_0^\circ(\mathrm{I}))/T$ / JK^{-1} mol^{-1}
		(Crystal-II)		
10	(1.05)	(0.332)	(0.249)	(0.083)
20	7.14	2.552	1.897	0.655
30	17.03	7.291	5.272	2.019
40	26.09	13.47	9.376	4.091
50	33.52	20.12	13.49	6.631
60	39.55	26.78	17.35	9.435
70	44.58	33.27	20.89	12.38
80	48.92	39.51	24.13	15.38
90	52.98	45.51	27.11	18.40
100	56.60	51.28	29.88	21.40
110	60.23	56.84	32.47	24.37
120	64.00	62.24	34.94	27.30
130	68.14	67.52	37.33	30.19
138.63		Transition		
		(Crystal-I)		
140	94.29	103.48	70.14	33.35
150	98.59	110.13	71.88	38.25
160	103.22	117.83	74.28	43.55
169.66		Fusion		
		(Liquid)		
170	115.08	142.46	95.51	46.95
180	117.23	149.13	96.68	52.45
190	118.92	155.51	97.05	58.46
200	120.89	161.66	98.91	62.75
210	123.00	167.61	100.01	67.60
220	125.32	173.38	101.10	72.28
230	127.73	179.01	102.21	76.80
240	130.49	184.50	103.33	81.17
250	133.30	189.89	104.47	85.41
260	136.18	195.17	105.64	89.54
270	139.13	200.37	106.82	93.54
280	142.31	205.48	108.03	97.45
290	145.57	210.53	109.27	101.26
300	148.98	215.52	110.54	104.99
		(Glassy and Supercooled Crystal-I)		
10	(1.75)	(12.27)	(275.58)	(−263.31)
20	10.90	15.96	140.71	−124.75
30	21.84	22.48	99.29	−76.81
40	30.43	30.02	81.07	−51.05
50	37.43	37.57	71.65	−34.08
60	43.20	44.92	66.44	−21.52
70	48.46	51.61	63.50	−11.89
80	61.34	58.98	62.51	−3.54
		(Crystal-III)		
10	(1.65)	(3.18)	(131.68)	(−128.50)
20	10.38	6.73	68.40	−61.67
30	21.08	13.01	50.89	−37.89
40	29.83	20.33	44.60	−24.27
50	36.82	27.75	42.36	−14.61
60	43.03	35.03	41.97	−6.94
70	49.00	42.13	46.42	−4.29
80	55.48	49.05	47.03	1.94
90	63.45	56.09	48.53	7.57
100	72.91	63.19	50.42	12.77

no residual entropy at 0 K. Taking this into consideration, the residual entropies of glassy crystal-I and glassy crystal-III were calculated. Contribution below 14 K was calculated by means of extrapolated heat capacities with a Debye model. The contribution from 85—140 K for crystal-I was calculated by the equations given in

Table 4. Details of the calculation are given in Table 5. The residual entropies of glassy crystal-I and glassy crystal-III were found to be (11.67±0.70) and (2.61±0.37) JK^{-1} mol^{-1}, respectively.

Thermodynamic Functions. Smoothed values of heat capacity at rounded temperatures along with values of other derived thermodynamic functions are given in Table 6. For all the phases, $H_0°$ refers to the zero point enthalpy of crystal-II. The entropy values for all phases are also referred to the entropy of crystal-II at 0 K, which is considered to be zero.

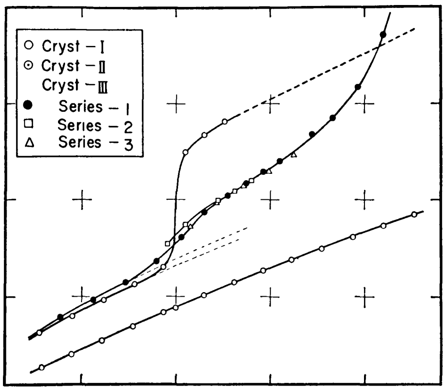

Fig. 4. Heat capacities of glassy crystal-I, -III and crystal-II around glass transition temperature.

Purity of the Crystal-III Phase. Heat capacity curves for crystal-I, -II, and -III around glass transition region are shown in Fig. 4. The temperatures at which the heat capacity jump occurs are very close for crystal-I and -III. Thus the possibility that the heat capacity jump for crystal-III is caused by crystal-I contained in crystal-III as an impurity might be considered. However, this possibility was discarded for the following reasons. (1) The results for series-1 and -3 agree in spite of the difference in the method of preparation of crystal-III. It is very improbable that different samples contain almost the same amount of impurity. (2) The ratios $S_0°$ (III)/$S_0°$ (I) (=0.22) and ΔC_p (III)/ΔC_p (I) (=0.32) differ from each other beyond the estimated error (ΔC_p is the heat capacity jump at around 80 K). (3) The activation enthalpies of the relaxation phenomena around glass transition region differ for crystal-I and crystal-III. (4) The heat capacity of crystal-III is greater in the temperature region 62—80 K. Our view that the heat capacity jump of crystal-III at around 80 K is an intrinsic property of this phase is thus supported.

Relaxation Around Glass Transition Region For both the glassy crystal-I and -III, heat evolution due to the enthalpy relaxation was observed to start at *ca.* 50 K, the temperature rising linearly with time (Fig. 5). If we assume an exponential type for the enthalpy relaxation, the following equation holds.

$$\frac{\mathrm{d}\Delta H(t)}{\mathrm{d}t} = -\frac{1}{\tau}\Delta H(t), \qquad (4)$$

where $\Delta H(t)$ is the enthalpy difference of the glassy state at time t and equilibrium state and τ the relaxation time. For small t ($t \ll \tau$), $\Delta H(t)$ is nearly equal to $\Delta H(0)$.

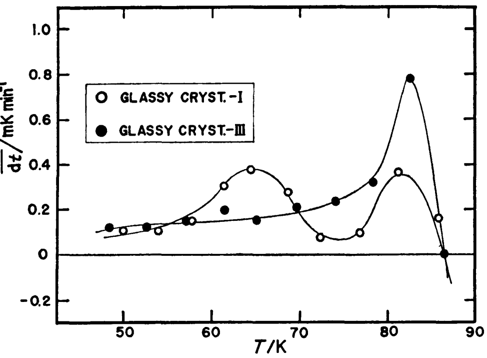

Fig. 5. Rate of the temperature rise at temperatures below T_g.

Thus, $\mathrm{d}\Delta H(t)/\mathrm{d}t$ is nearly constant, or the temperature of the sample rises linearly with time, the slope being proportional to $\Delta H(0)/\tau$. If a simple relaxation mechanism of the type of Eq. 4 is assumed, the behavior of the glassy crystal-III, in which one peak appears in $\mathrm{d}T/\mathrm{d}t$ *vs.* T curve, seems to be normal. No interpretation can be given for the origin of the second peak in the $\mathrm{d}T/\mathrm{d}t$ *vs.* T curve for glassy crystal-I. At temperatures above 78 K, the sign of the $\Delta H(0)$ changed, a negative temperature drift being observed. Relaxation times at various temperatures were determined by analysis of the drift by means of Eq. 4. From the Arrhenius plot of the relaxation time, the activation enthalpy of the relaxation was found to be 18 and 7 kJ mol^{-1} for glassy crystals -I and -III, respectively. The temperature at which the relaxation time for glassy crystal-I becomes one minute is found to be 92 K from this plot. The difference in the T_g values determined by the DTA method and heat capacity measurement might be explained by the difference in the time scale of the observation.

Preparation of Glassy Liquid by Vapor Condensation Method. DTA curves obtained with a vapor condensation type DTA apparatus are reproduced in Fig. 6. Run 1 is the heating curve of the sample condensed from vapor directly onto the sample holder maintained at 68 K. Runs 2 and 3 show the heating curves after the tempera-

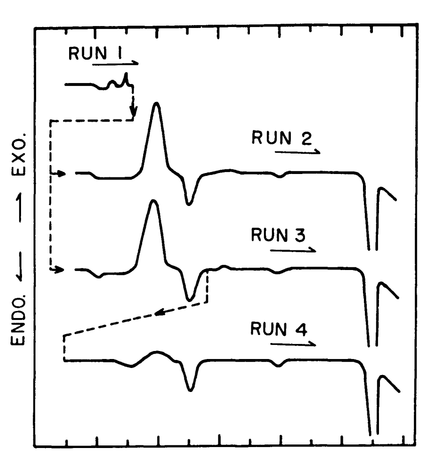

Fig. 6. DTA curves for the samples condensed from vapor.

ture cycling between 68 and 92 K. For Run 3 the sample was annealed for an hour at 77 K prior to the measurement. Run 4 shows the heating curve after the temperature cycling between 68 and 118 K and corresponds to Run 3 in Fig. 1. Although some exothermic anomalies in Run 1 cannot be assigned yet, there are evidences for concluding that each baseline shift to endothermic direction in these runs (Runs 1, 2, and 3) at 78 K is the manifestation of glass transition of liquid: (1) Annealing effect characteristic of the glass transition in Run 3. (2) Rough agreement of the liquid→crystal-III crystallization enthalpy ($=4.3\ \mathrm{kJ\ mol^{-1}}$) estimated from its peak area referring to the peak areas of crystal-III→crystal-I and melting of crystal-I with its value ($4.8\ \mathrm{kJ\ mol^{-1}}$) calculated from calorimetric data. It is tacitly assumed that the peaks in Run 1 do not represent the inherent property of a large part of the vapor condensed phase but that of the unstable crystalline phase formed as complex phase during the course of vapor condensation. Another interpretation that the peaks were caused by the transition occurring in all parts of the sample is also possible. If this is the case, the base line shift to endothermic direction in Run 1 corresponds to the glass transition of liquid but that in Runs 2 or 3 correspond to the glass transition of unstable new crystalline phase. We can conclude that the glassy liquid was prepared by the vapor condensation method, its glass transition temperature being 78 K.

Discussion

Molecular motions in crystalline state of cyclohexene were studied by Saffar *et al.*[11] by means of NMR. In their study on the temperature dependence of the second moment as well as of the spin lattice relaxation time, they found a phase transition at 128.5 K where we found no thermal anomaly. The lack of detailed description of the thermal treatment of their sample and the inconsistency between their assignment on the crystalline phases and ours make it difficult for us to discuss our results in reference to their work. A tentative interpretation is as follows.

Cyclohexene molecule has two half-chair conformations. The existence of another conformation (boat conformation) can be neglected in the low temperature region because of its high strain energy ($11.3\ \mathrm{kJ\ mol^{-1}}$ by Beckett *et al.*[10] and $18.0\ \mathrm{kJ\ mol^{-1}}$ by Anet[12]). Saffar *et al.*[11] reported that the ring inversion motion appears at 115 K in crystal-I (our nomenclature). Above this temperature the Arrhenius plot of the correlation time obtained from their T_1 experiment gave $10\ \mathrm{kJ\ mol^{-1}}$ for the activation energy which we obtained from the plot in Fig. 4 of their paper. Similarity of the value with the activation enthalpy of the relaxation phenomenon in crystal-III ($7\ \mathrm{kJ\ mol^{-1}}$) suggests that the ring inversion mode dominates the relaxation phenomenon of crystal-III near the glass transition region. It is plausible that this mode will survive down to a lower temperature than the life of molecular rotation because the energy difference giving rise to the ordering of the mode of such a ring inversion will be created with the settling down of the rotational motion. The energy difference between the two conformers also depends upon the packing density and symmetry of the crystal; higher density or the lower symmetry will give larger energy difference. It is likely that the energy difference in crystal-II, which seems to have higher density and lower symmetry, is so large that the order is attained at the transition temperature. On the other hand, the energy difference for crystal-III may be of the order of thermal energy, so the relaxation phenomenon of the ring inversion was observed calorimetrically. Complete disorder of the ring inversion mode should contribute to the entropy by $R\ln 2$ ($=5.8\ \mathrm{JK^{-1}\ mol^{-1}}$). Thus the partial order is already attained at T_g in crystal-III since the residual entropy of the glassy crystal-III ($2.7\ \mathrm{JK^{-1}\ mol^{-1}}$) is less than the value for complete disorder.

Since the residual entropy of glassy crystal-I is larger than $R\ln 2$, there must be some other type of disorder such as orientational randomness around the axis (z axis) normal to the molecular plane. The rotation about the axis was suggested by Saffar for crystal-I. The energy difference between the two conformers in crystal-I at T_g may be smaller than that of crystal-III at T_g' because of the more disordered orientational freedom, lower density, and presumably of the higher crystal symmetry of crystal-I. Mode of ring inversion in crystal-I seems to contribute to the residual entropy by the amount corresponding to nearly complete disorder.

Glassy crystals of cyclohexene seem to provide an interesting example for the simplification of the configurational mode. It is likely that the configurational freedom may be the rotation about z axis+ring inversion and simply ring inversion in crystal-I and crystal-III, respectively. If this is the case, the glass transition of crystal-III corresponds simply to the mode of ring inversion and successive simplification of the configurational freedom is achieved in the order of glassy liquid→glassy crystal-I→glassy crystal-III.

References

1) D. Turnbull and M. H. Cohen, *J. Chem. Phys.*, **31**, 1164 (1959); *ibid.*, **34**, 120 (1961).

2) J. H. Gibbs and E. A. DiMarzio, *J. Chem. Phys.*, **28**, 373 (1958).

3) C. A. Angell, *J. Phys. Chem.*, **75**, 3698 (1971).

4) K. Adachi, H. Suga, and S. Seki, *Bull. Chem. Soc. Jpn.*, **41**, 1078 (1968); **43**, 1916 (1970); **44**, 77 (1971); **45**, 1960 (1972).

5) H. M. Huffman, M. Eaton, and G. D. Oliver, *J. Am. Chem. Soc.*, **70**, 2911 (1948).

6) K. Adachi, H. Suga, and S. Seki, *Bull. Chem. Soc. Jpn.*, **43**, 1916 (1970).

7) O. Haida, H. Suga, and S. Seki, *Chem. Lett.*, **1973**, 79.

8) H. Suga and S. Seki, *Bull. Chem. Soc. Jpn.*, **38**, 1000 (1965).

9) O. Haida, H. Suga, and S. Seki, *Thermochimica Acta*, **3**, 177 (1972).

10) C. W. Beckett, N. K. Freeman, and K. S. Pitzer, *J. Am. Chem. Soc.*, **70**, 4227 (1948).

11) Z. M. Saffar, R. G. Eades, and J. P. Llewelly, *J. Chem. Phys.*, **50**, 3462 (1969).

12) F. A. L. Anet and M. Z. Hag, *J. Am. Chem. Soc.*, **87**, 3147 (1965).